

# The C-terminal lysines fine-tune P53 stress responses in a mouse model but are not required for stability control or transactivation

Kurt A. Krummel\*, Crystal J. Lee\*, Franck Toledo\*†, and Geoffrey M. Wahl\*\*

\*The Salk Institute for Biological Studies, Gene Expression Laboratory, 10010 North Torrey Pines Road, La Jolla, CA 92037; and †Institut Pasteur, Unite d'Expression Genetique et Maladies, 25 Rue du Dr. Roux, 75724 Paris Cedex 15, France

Edited by Inder M. Verma, The Salk Institute for Biological Studies, La Jolla, CA, and approved May 26, 2005 (received for review April 14, 2005)

**P53 is an unstable transcription factor that is mutated in a majority of human cancers. With a significant role in initiating cell elimination programs, a network has evolved to fine-tune P53 transcriptional output and prevent errant activation. Modifications of the C terminus have long been viewed as critical binary determinants of P53 stability or activation. However, these conclusions are based on *in vitro* transfection or biochemical analyses where the stoichiometries between P53 and its regulators are perturbed. Therefore, we tested the importance of the C-terminal regulatory region for P53 control in mice where the seven C-terminal lysines were changed to arginine (*Trp-53<sup>7KR</sup>*). Surprisingly, the homozygous mutant mice are viable and phenotypically normal. We have functionally characterized the mutant protein in both MEFs and thymocytes, revealing the unexpected result that *Trp-53<sup>7KR</sup>* exhibits a normal half-life and functions like WT P53 in cell cycle arrest and apoptosis, and in an E1A-ras xenograft tumor suppression assay. However, a significant difference is that P53<sup>7KR</sup> is activated more easily by DNA damage in thymus than WT P53. Importantly, although MEFs encoding WT P53 spontaneously emerge from crisis to become immortal in a 3T3 growth protocol, we do not observe any such escape with the P53<sup>7KR</sup> cells. We propose that the C-terminal modifications believed to be critical for proper P53 regulation are not essential, but contribute to a fine-tuning mechanism of homeostatic control *in vivo*.**

Mdm2 | p53 | tumor suppressor | Trp-53 | ubiquitination

**P**53 can respond to a variety of stimuli to either initiate cell cycle arrest or initiate apoptosis. Therefore, it is critical to control the output of this short-lived transcription factor (1). It is generally accepted that P53 regulation involves competition between the E3 ubiquitin ligase MDM2 and histone acetyl transferases (HATs). MDM2-mediated ubiquitination of the conserved C-terminal lysines of P53 initiates proteasome-dependent degradation, while the HATs acetylate the same lysines, resulting in P53 stabilization and activation (2, 3). Other studies report that C-terminal lysine methylation is required for P53 stabilization (4), neddylation inhibits transactivation (3), and sumoylation may have positive or negative roles (5). Regardless of the modification, the C terminus is thought to be critical for P53 stability or activation. However, these conclusions are often based on nonnative conditions, where the ratios between P53 and its regulators are altered. Therefore, we tested the importance of the C-terminal regulatory region for P53 control in mice where the seven C-terminal lysines were changed to arginine (*Trp-53<sup>7KR</sup>*).

## Methods

**Targeting Construct.** Using ET recombination (GeneBridges, Dresden Germany), we recovered the WT *Trp-53* locus from a 129 strain mouse BAC (a generous gift from Manuel Serrano, Spanish National Cancer Center, Madrid) with the following primers 5'-GAT AAG CAA GAC ATT GTA CCA GCA ATT AAC CCC CCA CCC CCA ACT CCA TAG CGG CCG CTG AAG ACG AAA GGG CCT CGT G-3', 5'-TGT TCT GAG CTC TGT GCT

CTT TCC TAT CCA GCT AGA TAG TCA TAG CCA TCC GAT CGG CGC TAG CGG AGT GTA TAC TGG C-3'. This fragment comprises the genomic sequence of *Trp-53* from 91 bp upstream of the beginning of exon 1 to 1,770 bp downstream of the last nucleotide of exon 11 in pACYC177 (NEB). The targeting construct contained extensive 5' homology upstream of exon 2 (BamHI), followed by exons 2–10, then Exon 11 with the *Trp-53<sup>7KR</sup>* mutation to the 3' EcoRV site. The positive selection cassette fragment containing loxP-neo-loxP, from a modified pOG277 plasmid (6), follows the *Trp-53<sup>7KR</sup>* mutation. The neo cassette introduces an additional EcoRI site that was used for Southern blot analyses. After the Neo cassette, 1.3 kb of *Trp-53* 3' homology is present (EcoRV–ClaI). Finally, the thymidine kinase negative selection cassette is derived from the plasmid pNT and follows the 3' homology region. Our final construct was assembled in pSP72N (Promega). Each exon, the intron–exon boundary, the neo and TK cassettes, and the entire 3' homology region were sequenced to ensure *Trp-53* status.

**Homologous Recombination and Genotyping.** PrmCre 129/SvJae ES cells (6) were electroporated with the linearized targeting construct. We screened G-418 and ganciclovir-resistant colonies for the presence of the EcoRI restriction site within the Neo cassette by using Southern blot hybridization of EcoRI-digested DNA with a 500-bp fragment 5' (Eco0109I/StyI) and a 382-bp fragment 3' (EcoRV/NotI) to the targeting construct as probes. Southern blotting was performed as described (7). Of 192 doubly resistant ES cell clones, 29 candidates were identified. The presence of the mutation was confirmed independently by PCR amplification in nine clones using primers flanking the mutation region 5'-TGG TGG TGG TGA CAG TTG TG-3', 5'-TCT CAG CCC TGA AGT CAT AAG-3'. The resulting PCR fragments were then digested with Bsu36I, because the 7KR mutation introduces this site. After digestion, a smaller band indicates the presence of the mutant. Two separate ES clones containing the targeted *Trp-53<sup>7KR</sup>* allele were injected into blastocysts, which were then implanted into pseudo-pregnant females. Germ-line transmission was verified by genotyping MEFs from the breeding of two chimeras with *Trp-53<sup>+/-</sup>* mice. RNA was isolated from *Trp-53<sup>7KR/-</sup>* MEFs, and we used a RT-PCR strategy to verify that the sequence was identical to the WT *Trp-53* sequence except for the 7KR mutation. The chimeras were also bred to C57BL/6 *Trp-53* mice to produce *Trp-53<sup>+/7KR</sup>* offspring. These offspring were genotyped, then interbred to produce homozygous mutant MEFs and mice. The *Trp-53<sup>+/7KR</sup>* mice were also backcrossed to C57BL/6 mice for functional studies to reflect the standard genetic background of *Trp-53* mutant animals.

**Cell Culture.** Primary MEFs were isolated from 13.5-day-old embryos, genotyped, and cultured in DMEM with 15% FBS,

This paper was submitted directly (Track II) to the PNAS office.

†To whom correspondence should be addressed. E-mail: wahl@salk.edu.

© 2005 by The National Academy of Sciences of the USA



$\alpha$ -actin (Sigma). Secondary antibodies used include peroxidase-conjugated goat anti-mouse IgG and anti-rabbit IgG (Pierce). Probed blots were incubated with Pierce Supersignal West Pico chemiluminescent substrate. Blots were exposed to x-ray films.

**Ubiquitination.** Ubiquitination was detected as described (9). Briefly, we transfected MEFs that are deleted for both *Trp-53* and *Mdm2* with exogenous *Trp-53* or *Trp-53<sup>7KR</sup>*, *Mdm2*, and His-ubiquitin. Cells were cultured for 24 h, then MG132 was added for an additional 3 h to one replicate sample of each genotype. We lysed the cells under conditions that prevent deubiquitination, and purified the lysates with Ni-agarose, performed SDS/PAGE, and immunoblotted for P53.

**Quantitative PCR.** Total RNA was extracted by using RNeasy mini kit (Qiagen, Valencia, CA) and reverse transcribed by using Superscript III RT (Invitrogen). Real-time quantitative PCR was performed on an Applied Biosystems PRISM 7700 sequence detection system using Platinum SYBR Green mastermix (Invitrogen). Primer sequences are available upon request for detecting cDNA sequence of *Trp-53*, *p21*, *Mdm2*, *Noxa*, and *Puma*, and control genes *H6pd* and *Hprt*.

**Flow Cytometry.** For cell cycle analyses, log phase cells were irradiated with 0.5, 2, or 6 Gy  $\gamma$  irradiation and incubated for 24 h. Cells were then pulse-labeled for 1 h with BrdUrd (10  $\mu$ M), fixed in 70% ethanol, and stained with FITC anti-BrdUrd and propidium iodide as described (7). Apoptosis assays were performed on E1A expressing MEFs that were treated for 24 h with 0.25  $\mu$ g/ml adriamycin or treated in culture with varying doses of  $\gamma$  irradiation. Thymocytes were isolated from mice exposed to whole-body irradiation at varying doses from a Co-60 source. The treated cells were harvested and stained with Annexin-V-FITC for analysis. For both cell cycle and apoptosis, the cells were sorted by using a Becton Dickinson FACScan machine, and data were analyzed by using Becton Dickinson CELLQUEST PRO, or WINMDI 2.8.

## Results and Discussion

We generated a mouse model of *Trp-53* with C-terminal lysine mutations, shown by transfection studies to be stable and transcriptionally active (2, 10) (Fig. 1 *a* and *b*). Because the mouse *Trp-53* gene contains seven lysines in the C terminus, all were changed to arginine (*Trp-53<sup>7KR</sup>*). The sequence-confirmed construct (see *Methods*) was linearized and electroporated into PrmCre ES cells to allow excision of the Neo cassette upon passage through the male germ line, and putative recombinants were screened by both Southern blotting and allele-specific PCR (Fig. 1 *c* and *d*) (6, 7). Two homologous recombinant ES clones (designated B52 and B54) were injected into C57BL/6 blastocysts to produce *Trp-53<sup>7KR</sup>* chimeras and *Trp-53<sup>+/7KR</sup>* mice. Transcription of the WT and *Trp-53<sup>7KR</sup>* alleles were equivalent by quantitative RT-PCR analysis (data not shown). The entire *Trp-53* coding region from *Trp-53<sup>7KR/7KR</sup>* MEFs was sequenced and found to be WT at all codons except for the expected mutations of the seven C-terminal lysines (Fig. 6, which is published as supporting information on the PNAS web site) (11).

Expectations based on the stability and hyperactivity of the human P53<sup>6KR</sup> protein suggested the possibility of early embryonic lethality, as observed in both *Mdm2* and *MdmX* knockout mice (12, 13). However, *Trp-53<sup>7KR/7KR</sup>* animals were physically indistinguishable from their WT (i.e., *Trp-53*) littermates, and the Mendelian ratio of *Trp-53<sup>7KR/7KR</sup>* and *Trp-53<sup>+/7KR</sup>* mice was normal.

The apparent normality of the *Trp-53<sup>7KR</sup>* mice was unexpected, leading us to thoroughly evaluate the properties of the encoded protein. Immunofluorescence analyses revealed that, during exponential growth and after adriamycin induced DNA damage, the subcellular localization and abundance of P53 and P53<sup>7KR</sup> appeared equivalent (Fig. 7, which is published as supporting information on

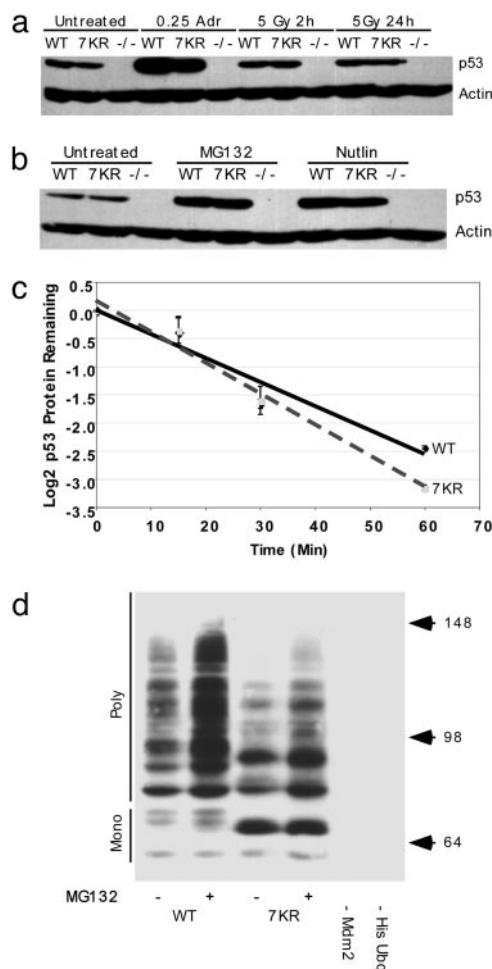


**Fig. 2.** P53<sup>7KR</sup> protein abundance, stabilization, half-life, and ubiquitination are similar to WT. (a) Western blot to determine *Trp-53* protein levels in early passage MEFs in culture. MEFs less than passage 5 were treated with 0.25  $\mu$ g/ml adriamycin for 24 h, followed by SDS/PAGE and detection with the anti-P53 antibody (CM-5). Alternatively, cells were treated with 5 Gy  $\gamma$  irradiation, then allowed to recover for either 2 or 24 h before lysis. Actin is shown as a loading control. (b) Western blot detection of P53 in cells treated with the 10  $\mu$ M proteasome inhibitor MG132 or 10  $\mu$ M Nutlin for 4 h. (c) Determination of P53 half-life in early passage MEFs. MEFs were treated with 100  $\mu$ g/ml cycloheximide for the times indicated, then analyzed by Western blot. *Trp-53* was detected with either CM-5 or Ab7, and actin was used as a loading control. P53 and actin were quantitated by using IMAGEQUANT. (d) Ubiquitination detection in P53/MDM2 deficient cells was performed as described (9). From left to right, His-ubiquitin and Mdm2 were introduced with exogenous *Trp-53* (lanes 1 and 2) or *Trp-53<sup>7KR</sup>* (lanes 3 and 4). After 24 h, 30  $\mu$ M MG132 was added for 3 h (lanes 2 and 4), and cells were lysed. Lane 5 contains *Trp-53* and His-ubiquitin without Mdm2. Lane 6 contains P53 and MDM2 without His-ubiquitin. Lysates were incubated with Ni-Agarose to bind His-ubiquitinated proteins. After several washes, bound proteins were eluted and SDS/PAGE was performed. Finally, we performed Western blot detection of P53 with CM-5 on the purified proteins. Molecular weights are indicated on the right.

the PNAS web site). More precise quantifications of protein levels by Western blotting demonstrate that WT and P53<sup>7KR</sup> levels in normally growing early passage MEFs are similar, and that their increases in response to  $\gamma$  irradiation and adriamycin are equivalent (Fig. 2*a*).

P53 levels are largely determined by MDM2-dependent proteasomal degradation (14). The proteasome inhibitor MG132 led to equivalent increases in the levels of WT and P53<sup>7KR</sup>, implying that their steady state levels are largely determined by proteasome-dependent processes. However, this result does not indicate the

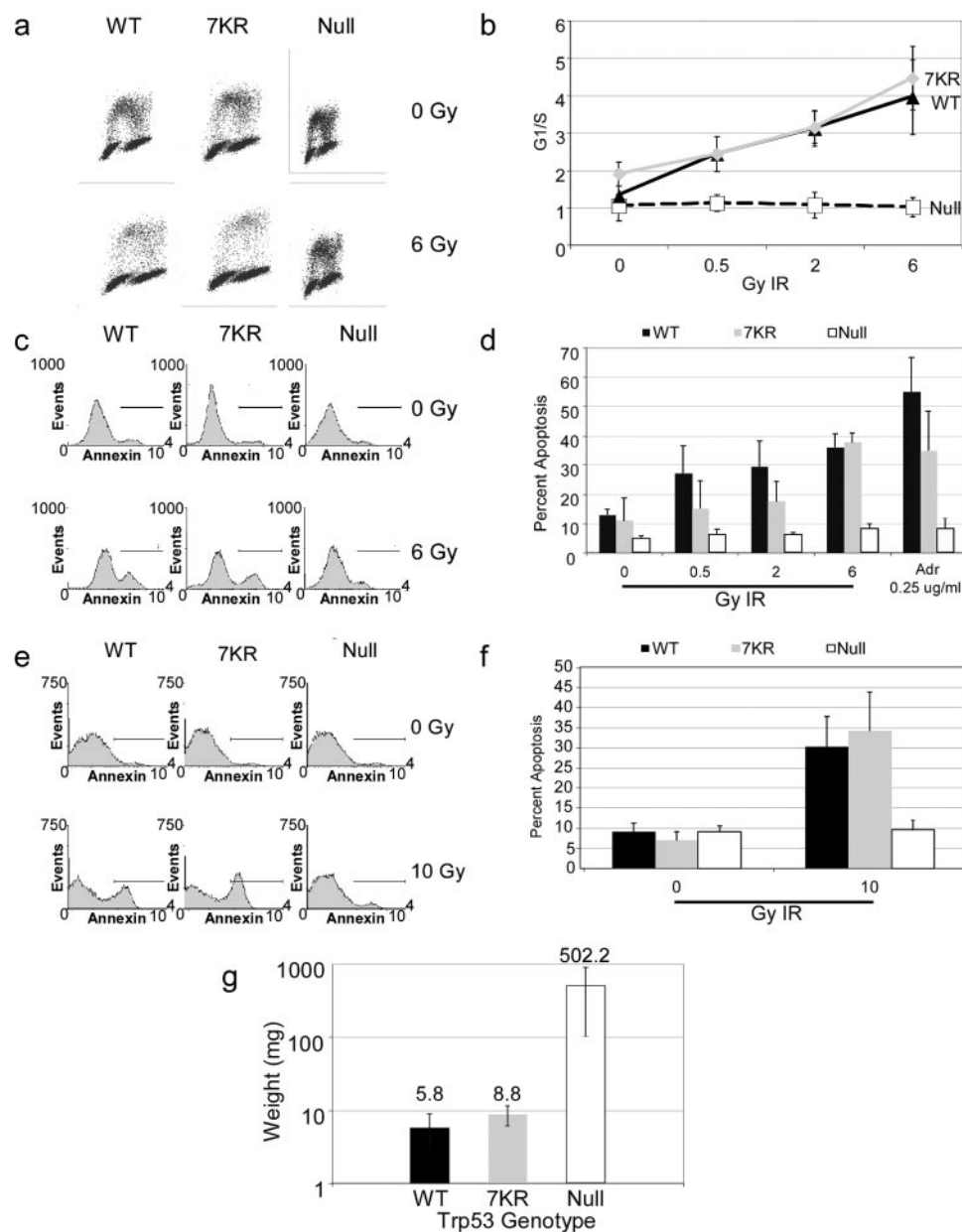


**Fig. 3.** Cell cycle and apoptosis response of P53<sup>7KR</sup> is normal in MEFs and thymocytes. (a) Cell cycle arrest analysis in MEFs. Asynchronous cell populations of *Trp-53<sup>null</sup>*, *Trp-53*, and *Trp-53<sup>7KR</sup>* MEFs were untreated or treated with 6 Gy  $\gamma$  irradiation, then analyzed by FACS after 24 h. A representative experiment for cells of each genotype is shown. (b) Cell cycle arrest analysis summary. The graph shows the G<sub>1</sub>/S ratios and SD from at least four independent experiments for each genotype from independent MEFs. (c) Analysis of apoptosis *in vitro*. Asynchronous cultures of E1A expressing *Trp-53<sup>-/-</sup>*, *Trp-53*, and *Trp-53<sup>7KR</sup>* MEFs were untreated or treated with 6 Gy  $\gamma$  irradiation, and analyzed for apoptosis after 24 h by staining with Annexin-FITC and FACS. A representative experiment for cells of each genotype is shown. (d) Analysis of apoptosis in E1A-MEFs. The bar graph shows the mean percentage of apoptotic cells and the SD from at least three independent experiments for each genotype with independent MEFs. Asynchronous cultures of E1A expressing *Trp-53<sup>-/-</sup>*, *Trp-53*, and *Trp-53<sup>7KR</sup>* MEFs were untreated or treated with various doses of  $\gamma$  irradiation, or 0.25  $\mu$ g/ml adriamycin, then analyzed after 24 h by staining with Annexin-FITC and FACS. (e) Analysis of apoptosis *in vivo*. In four independent experiments, mice were untreated or exposed to 10 Gy whole-body irradiation. After 4 h, we measured the percentage of apoptotic thymocytes. Each experiment consisted of two mice for each genotype (*Trp-53<sup>null</sup>*, *Trp-53*, and *Trp-53<sup>7KR</sup>*), one untreated and one irradiated. Representative FACS data are plotted. (f) Summary of *in vivo* apoptosis data. The mean percentage of apoptotic cells and SD from the experiments are shown. Black bars, WT P53; gray bars, P53<sup>7KR</sup>; empty bars, P53<sup>null</sup>. (g) Xenograft assay of tumorigenicity. Equal numbers of E1A and Ras expressing MEFs of the indicated genotypes were injected into the flanks of nude mice and tumors were allowed to grow for 14 days. Mice were killed, and the weight of tumors was determined. Results are expressed as the weight of age-matched tumors. Mean and SD were calculated from six tumors for each genotype. Note that the y axis is a logarithmic scale.

extent to which P53<sup>7KR</sup> stability is regulated by MDM2 because additional ubiquitin ligases have recently been reported to mediate p53 degradation (14). Therefore, we used Nutlin to determine its effects on the abundance of WT and P53<sup>7KR</sup> (15). We investigated the specific contribution of MDM2 to P53<sup>7KR</sup> destabilization by using Nutlin, a small molecule that selectively inhibits the P53-

MDM2 interaction by binding to MDM2 in the P53-binding pocket. Nutlin induced similar levels of accumulation for both WT and P53<sup>7KR</sup> proteins (Fig. 2b). This finding indicates that P53<sup>7KR</sup> protein degradation is determined primarily by MDM2, especially because Nutlin is unlikely to affect binding of another ubiquitin ligase for P53, such as PIRH2, which binds to a different region of P53 (16).

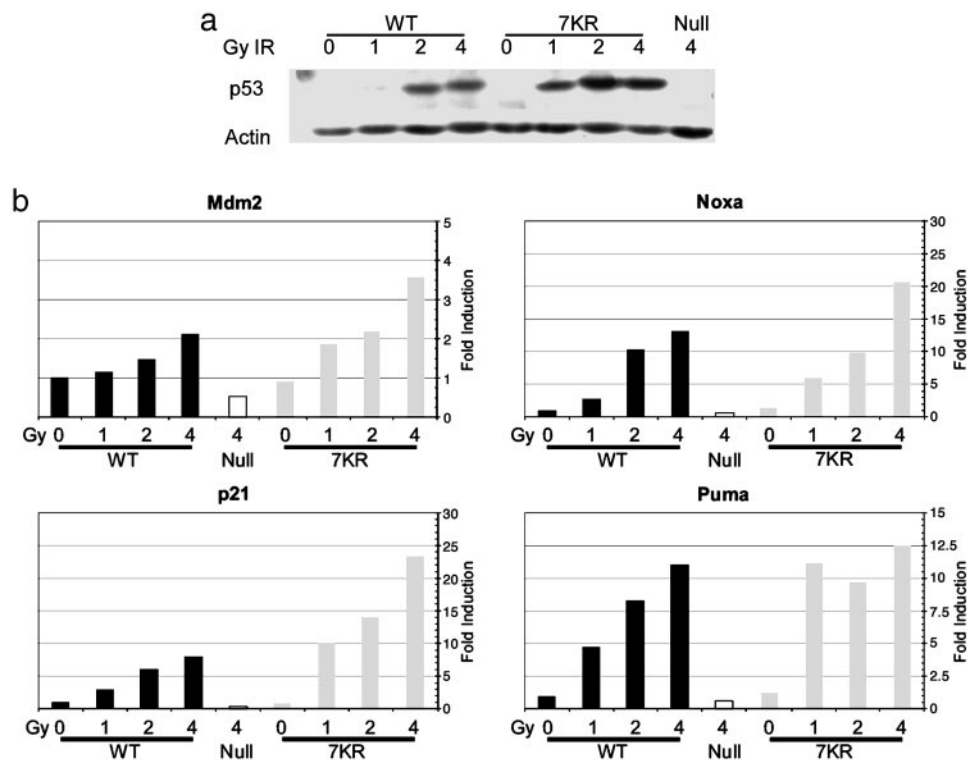


**Fig. 4.**  $\gamma$  irradiation in thymus reveals a sensitized transcriptional response of P53<sup>7KR</sup>. (a) P53 protein induction after  $\gamma$  irradiation. WT P53, P53<sup>7KR</sup>, and P53<sup>null</sup> mice were left untreated or submitted to increasing doses of  $\gamma$  irradiation as indicated. After 3 h, thymi were removed, and protein extracts were prepared for Western blot. P53 was detected with CM-5, and actin is used as a loading control. (b) Transcriptional analysis of P53 target genes *in vivo*. The thymi used for Western blot detection of P53 levels in a were divided and analyzed by QPCR for the four P53 target genes shown. Treatments for all genotypes are depicted relative to untreated WT P53, which is set to 1. WT P53 is shown in black bars, and P53<sup>7KR</sup> is shown in gray bars. For P53<sup>null</sup>, only the response to 4-Gy irradiation is shown (empty bars). The data represent the results of duplicate experiments.

These data contrast with previous transfection assays indicating that the human 6KR mutant is resistant to MDM2-mediated degradation (2). However, we observed that cotransfection of either MDM2 or HDM2 with human WT P53 or the 6KR mutant resulted in similar extents of degradation of both proteins (data not shown). Therefore, as in the mouse, mutation of the human C-terminal lysines does not generate an MDM2-resistant P53.

To directly address the stability of P53<sup>7KR</sup>, the protein half-lives of P53<sup>7KR</sup> and WT were compared in early passage MEFs treated with the protein synthesis inhibitor cycloheximide. In accord with the data reported above, the half-life of P53<sup>7KR</sup> was  $\approx$ 20 min, which is equivalent to that of WT and consistent with numerous previous studies (Fig. 2c) (17). This finding is in stark contrast to the prediction that the seven C-terminal lysines are critical for P53 degradation.

Proteasomal degradation requires the addition of a ubiquitin chain on at least one lysine (14), or by recently reported ubiquitin-independent mechanisms (18, 19). Therefore, we determined whether P53<sup>7KR</sup> is ubiquitinated. Attempts to detect endogenous ubiquitination on WT or P53<sup>7KR</sup> were unsuccessful, even in the presence of exogenous Mdm2 and proteasome inhibition (data not shown). However, transfecting exogenous *Trp-53*, *Mdm2*, and His-ubiquitin into MEFs deleted for both *Trp-53* and *Mdm2* enabled detection of ubiquitinated WT and P53<sup>7KR</sup> (Fig. 2d). Importantly, the ubiquitination patterns are qualitatively different. It is unclear which of the ubiquitinated molecules contain multiple mono- or polyubiquitinations (20), but MG132 increases many of the higher molecular weight ubiquitinated species for WT, and not for P53<sup>7KR</sup>. A reasonable interpretation is that these bands correspond to ubiquitination of the seven C-terminal lysines. Although no increase as dramatic as this is observed in the P53<sup>7KR</sup> lane, MG132

treatment does increase some ubiquitinated species, implying instability of the corresponding P53<sup>7KR</sup> molecules.

The induction of cell cycle arrest and apoptosis are two *Trp-53* functions critical for tumor suppression, and C-terminal acetylation has been suggested to be important for the execution of both. Analysis of the cell cycle arrest response in MEFs exposed to increasing doses of ionizing radiation revealed the previously reported lack of cell cycle arrest in *Trp-53<sup>null</sup>* cells exposed to high radiation doses. However both *Trp-53* and *Trp-53<sup>7KR</sup>* MEFs exhibited significant decreases in the S-phase fraction and increases in G<sub>1</sub> content (Fig. 3a and b). MEFs with *Trp-53* are refractory to apoptosis and instead undergo G<sub>1</sub> arrest (21). To analyze the apoptotic potential of P53<sup>7KR</sup>, we infected MEFs with the E1A oncogene to sensitize them to apoptosis after DNA damage (22). Whereas *Trp-53<sup>null</sup>* MEFs exhibited little detectable apoptosis under these conditions, *Trp-53* and *Trp-53<sup>7KR</sup>* E1A-MEFs exhibited equivalent and substantial apoptotic levels (Fig. 3c and d). Furthermore, analyses of apoptosis in thymi isolated directly from irradiated mice again demonstrated the response to be largely P53 dependent and equivalent in both *Trp-53* and *Trp-53<sup>7KR</sup>* animals at all radiation doses used (Fig. 3e and f, and data not shown).

We estimated the tumor suppressive capacity of each P53 allele by infecting MEFs of each genotype with retroviruses encoding the E1A and Ras oncogenes, followed by injection of the resulting cells into the flanks of nude mice (7). Injections of E1A-Ras *Trp-53<sup>null</sup>* MEFs produced large, rapidly growing tumors, whereas E1A-Ras MEFs expressing either WT or P53<sup>7KR</sup> generated very small masses (Fig. 3g). We infer that the tumor suppressive function of P53<sup>7KR</sup> is equivalent to that of WT using this xenograft assay.

In contrast to the prediction of hyperactivity of P53<sup>7KR</sup>, based on *in vitro* studies, the above results suggest that WT and P53<sup>7KR</sup> are

functionally equivalent. We directly analyzed transcriptional output of both alleles *in vitro* in MEFs and *in vivo* in thymocytes. In agreement with the Western blot and functional analyses, target gene induction by P53<sup>7KR</sup> was similar to that of WT in MEFs. However, we have often noted high basal activities for both alleles in putatively unstressed cells in culture, perhaps as a response to high oxygen or other cell culture related stresses. To eliminate such variables, we analyzed the irradiation dose-response of WT and P53<sup>7KR</sup> in mouse thymocytes. In contrast to what was observed in MEFs, Western blot analysis showed that P53<sup>7KR</sup> protein was stabilized at a dose of 1 Gy, whereas WT protein remained undetectable. Furthermore, at all radiation doses analyzed, P53<sup>7KR</sup> was more abundant than WT (Fig. 4a). Consistent with these results, transactivation of the P53 target genes *p21*, *Mdm2*, *Puma*, and *Noxa* by quantitative PCR (Fig. 4b) demonstrated that P53<sup>7KR</sup> elicited more robust target gene induction than WT. Therefore, *in vivo*, *Trp-53*<sup>7KR</sup> encodes a protein that is more easily induced and activated than *Trp-53*, although the difference is more modest than suggested by *in vitro* analyses.

Each of the assays reported above is limited in that an acute function of P53 is evaluated. To assess the effects of P53 activity over a prolonged time period, we determined the consequences of *Trp-53* and *Trp-53*<sup>7KR</sup> expression by using an *in vitro* 3T3 immortalization protocol (23). Over time, *Trp-53* MEFs exhibited increased doubling time, entered crisis, and emerged as immortal variants (24) (Fig. 5a). *Trp-53*<sup>null</sup> MEFs grew more rapidly than *Trp-53* MEFs, failed to enter crisis, and spontaneously immortalized (Fig. 5a). By contrast, *Trp-53*<sup>7KR</sup> MEF grew at about the same rate as *Trp-53* until passage 7, then slowed down, and senesced consistently at approximately passage 10 (Fig. 5a). As seen in Fig. 5b, by passage 12, *Trp-53*<sup>7KR</sup> MEFs exhibited a senescent “fried egg” morphology, increased cell size, and failure to increase in number. Therefore, the elevated activity of P53<sup>7KR</sup> is manifested over numerous generations *in vitro* by a predisposition to an apparently irreversible senescence.

The fact that P53<sup>7KR</sup> has the same abundance and half-life as endogenous WT disproves the model that ubiquitination of P53 C-terminal lysines directly determines its degradation. There are several alternative possibilities for the regulation of P53 stability. First, it is possible that ubiquitination of alternative sites by MDM2 can mediate P53 degradation, but those in the C terminus are preferred or more accessible. An alternative explanation stems from the observation that some proteins are degraded by the proteasome without a requirement for their own ubiquitination (18, 19). This raises the formal possibility that mere association of ubiquitinated MDM2 with P53 may be sufficient for degradation of the entire complex by the proteasome. Our findings also disprove the model that C-terminal lysine acetylation or other modifications are required for function. Indeed, our data show that in the absence of a capacity for C-terminal lysine modifications, P53<sup>7KR</sup> is equally or more active than WT.

Therefore, these data suggest that the C-terminal lysines may have evolved to enable the fine-tuning of P53 activity over the

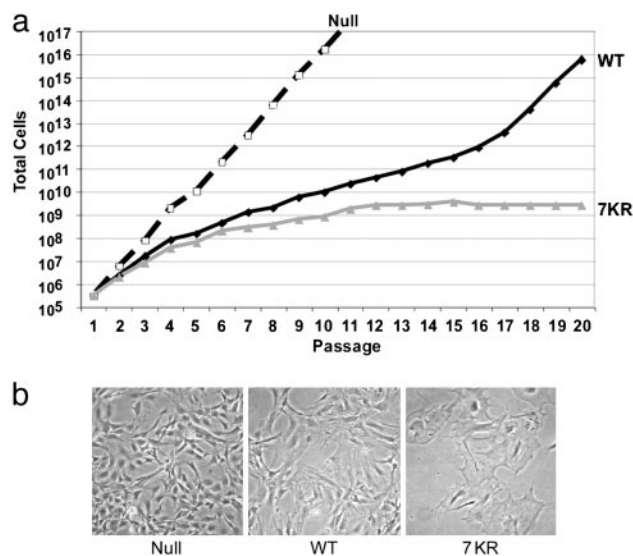


**Fig. 5.** P53<sup>7KR</sup> MEFs exhibit an increased sensitivity to culture stress in a 3T3 protocol. (a) Analysis of immortalization using a 3T3 growth protocol. A representative graph showing sensitivity to senescence by P53<sup>7KR</sup> MEFs is displayed. WT P53 (black diamonds), P53<sup>null</sup> (empty squares), and P53<sup>7KR</sup> (gray triangles) MEFs were freshly isolated from embryos 13.5 days postcoitum, counted, and serially passaged at  $3 \times 10^5$  cells in duplicate every 3 days for up to 20 passages. (b) Representative images are shown from passage 12 MEFs showing P53<sup>7KR</sup> cells displaying a senescence-like morphology.

lifespan of the metazoans in which it functions. For example, without C-terminal ubiquitination, perhaps P53<sup>7KR</sup> is cleared less efficiently from target gene promoters, enabling more efficient target gene activation than WT. In MEFs passaged *in vitro*, this activation is not detectable, but in longer term analyses involving exposure to more subtle stresses, or *in vivo*, the importance of these residues is manifested.

Finally, our data regarding P53 stability control may have broad implications for the regulation of numerous other short-lived transcription factors whose degradation is mediated by interaction with ubiquitin ligases. Although P53 has been intensively studied for many years by using *in vitro* models, our studies raise questions about the applicability of the mechanisms deduced from these studies for regulating P53 stability and function *in vivo*.

We thank Lyubomir Vassilev for the invaluable Nutlin reagents, J. Rossant for LIF, A. Francis Stewart (University of Technology, Dresden, Germany) for ET Recombination, Manuel Serrano for the mouse BAC used in producing our construct, and Mark Wade for many helpful discussions. This work was supported by National Cancer Institute Grants CA100845 and CA61449 (to G.M.W.), National Institutes of Health Grant 5 T32 CA009370-23 (to K.A.K.), and a fellowship from the Association pour la Recherche sur le Cancer (to F.T.).

1. Wahl, G. M., Stommel, J. M., Krummel, K., & Wade, M. (2005) in *25 Years of P53 Research*, eds. Hainaut, P. & Wiman, K. (Springer, Berlin), p. 446.
2. Rodriguez, M. S., Desterro, J. M., Lain, S., Lane, D. P., & Hay, R. T. (2000) *Mol. Cell Biol.* **20**, 8458–8467.
3. Xirodimas, D. P., Saville, M. K., Bourdon, J. C., Hay, R. T., & Lane, D. P. (2004) *Cell* **118**, 83–97.
4. Chuiikov, S., Kurash, J. K., Wilson, J. R., Xiao, B., Justin, N., Ivanov, G. S., McKinney, K., Tempst, P., Prives, C., Gambelin, S. J., et al. (2004) *Nature* **432**, 353–360.
5. Muller, S., Ledl, A., & Schmidt, D. (2004) *Oncogene* **23**, 1998–2008.
6. O’Gorman, S., Dagenais, N. A., Qian, M., & Marchuk, Y. (1997) *Proc. Natl. Acad. Sci. USA* **94**, 14602–14607.
7. Jimenez, G. S., Nister, M., Stommel, J. M., Beeche, M., Barcarse, E. A., Zhang, X. Q., O’Gorman, S., & Wahl, G. M. (2000) *Nat. Genet.* **26**, 37–43.
8. Jones, S. N., Sands, A. T., Hancock, A. R., Vogel, H., Donehower, L. A., Linke, S. P., Wahl, G. M., & Bradley, A. (1996) *Proc. Natl. Acad. Sci. USA* **93**, 14106–14111.
9. Xirodimas, D., Saville, M. K., Edling, C., Lane, D. P., & Lane, S. (2001) *Oncogene* **20**, 4972–4983.
10. Luo, J., Su, F., Chen, D., Shiloh, A., & Gu, W. (2000) *Nature* **408**, 377–381.
11. Jimenez, G. S., Nister, M., Beeche, M., Stommel, J. S., Barcarse, E., O’Gorman, S., & Wahl, G. M. (2005) *Nat. Genet.* **37**, 205.
12. Jones, S. N., Roe, A. E., Donehower, L. A., & Bradley, A. (1995) *Nature* **378**, 206–208.

13. Migliorini, D., Denchi, E. L., Danovi, D., Jochemsen, A., Capillo, M., Gobbi, A., Helin, K., Pelicci, P. G., & Marine, J. C. (2002) *Mol. Cell Biol.* **22**, 5527–5538.
14. Brooks, C. L., & Gu, W. (2004) *Cell Cycle* **3**, 895–899.
15. Vassilev, L. T., Vu, B. T., Graves, B., Carvajal, D., Podlaski, F., Filipovic, Z., Kong, N., Kammlott, U., Lukacs, C., Klein, C., Fotouhi, N., & Liu, E. A. (2004) *Science* **303**, 844–848.
16. Leng, R. P., Lin, Y., Ma, W., Wu, H., Lemmers, B., Chung, S., Parant, J. M., Lozano, G., Hakem, R., & Benchimol, S. (2003) *Cell* **112**, 779–791.
17. Moll, U. M., & Petrenko, O. (2003) *Mol. Cancer Res.* **1**, 1001–1008.
18. Chen, X., Chi, Y., Bloecher, A., Aebersold, R., Clurman, B. E., & Roberts, J. M. (2004) *Mol. Cell Biol.* **24**, 839–847.
19. Bossis, G., Ferrara, P., Acquaviva, C., Jariel-Encontre, I., & Piechaczyk, M. (2003) *Mol. Cell Biol.* **23**, 7425–7436.
20. Li, M., Brooks, C. L., Wu-Baer, F., Chen, D., Baer, R., & Gu, W. (2003) *Science* **302**, 1972–1975.
21. Kastan, M. B., Zhan, Q., el-Deiry, W. S., Carrier, F., Jacks, T., Walsh, W. V., Plunkett, B. S., Vogelstein, B., & Fornace, A. J., Jr. (1992) *Cell* **71**, 587–597.
22. Lowe, S. W., Ruley, H. E., Jacks, T., & Housman, D. E. (1993) *Cell* **74**, 957–967.
23. Todaro, G. J., & Green, H. (1963) *J. Cell Biol.* **17**, 299–313.
24. Parrinello, S., Samper, E., Krtolica, A., Goldstein, J., Melov, S., & Campisi, J. (2003) *Nat. Cell Biol.* **5**, 741–747.